Andrej Cibicik[1]
Department of Mechanical and Industrial Engineering,
Norwegian University of Science and Technology (NTNU),
N-7491 Trondheim, Norway
e-mail: andrej.cibicik@ntnu.no

Geir O. Tysse
Department of Mechanical and Industrial Engineering,
Norwegian University of Science and Technology (NTNU),
N-7491 Trondheim, Norway
e-mail: geir.o.tysse@ntnu.no

Olav Egeland
Department of Mechanical and Industrial Engineering,
Norwegian University of Science and Technology (NTNU),
N-7491 Trondheim, Norway
e-mail: olav.egeland@ntnu.no

Determination of Reaction Forces of a Deck Crane in Wave Motion Using Screw Theory

In this paper, we present a method for calculating reaction forces for a crane mounted on a ship moving in waves. The method is used to calculate the reaction forces between the crane base and the vessel deck. This includes the case where the crane is mounted on the platform that keeps the base of the crane horizontal when the vessel is moving in roll and pitch. The wave motion of the ship is modeled with force response amplitude operators (RAOs) based on the JONSWAP wave spectrum. The combined equations of motion for a vessel and a crane are derived using Kane's equations of motion, where velocities and angular velocities are formulated in terms of twists, and the associated partial velocities and partial angular velocities are given as lines in Plücker coordinates. The unknown reaction forces are represented as wrenches and are determined using screw transformations. The method is used to study the effect of the roll and pitch compensation platform in numerical simulations. The efficiency of the platform is evaluated in terms of the magnitude of reaction forces and crane payload sway angles. [DOI: 10.1115/1.4043701]

1 Introduction

Crane operations are important in the offshore industry as a vital element in the supply chain of offshore installations. Offshore cranes may be large and heavy structures, which apply significant dynamic reaction forces and moments to the structure of the vessel. For small vessels, the mass of a crane may be significant compared to the mass of the vessel, which means that the motion of the crane will influence the motion of the ship. In such cases, it will be useful to determine the reaction forces from a dynamic analysis, where the equations of motion for the combined crane and vessel system are used. The determined reaction forces will be needed in the design of the connection between the crane and the deck. Alternatively, the reaction forces can be used to determine the design specifications for a roll and pitch compensation platform, when it is used to keep the base of the crane horizontal, while the vessel is moving in waves. The dynamic analysis based on the combined equations of motion can be used to determine the reaction forces for the cases with and without the motion compensation platform, which may be useful for the evaluation of the platform efficiency.

The dynamic coupling between crane load and vessel motion was studied in Ref. [1] for a floating crane barge. The response of the barge was found when the barge and the crane are modeled as one rigid body. A simulator for a vessel with a crane was presented in Ref. [2], where the authors used an object-oriented modeling approach and co-simulation with the functional mock-up interface [3].

The combined dynamics of a ship and a deck crane were derived in Ref. [4], where Lie Groups and Lagrangian mechanics were used to derive the equations of motion for a general vehicle-manipulator system where the vehicle has six degrees-of-freedom (DOFs). Earlier work on the same topic was presented in Ref. [5], where the equations of motion of a spacecraft-manipulator system were derived using Kane's equation of motion. Kane's equations of motion [6] for multibody systems are based on the Newton–Euler formulation, where the forces of constraints are eliminated using the principle of virtual work. In Kane's method, the principle of virtual work is formulated in terms of partial velocities and partial angular velocities, which serve as projection operators that project inertial and external forces onto the directions associated with the generalized speeds. In this way, a minimal set of ordinary differential equations is obtained. Kane's method was originally formulated at the component level using coordinate-free vectors [6], and it was used in a very detailed derivation of the equations of motion for a Stanford manipulator in Ref. [7]. An alternative formulation of Kane's equations of motion for serial-link mechanisms was achieved by Angeles and Ma [8], where a matrix formulation was introduced using the link twists to determine the projection operators in the form of a natural orthogonal complement. This was further developed in Ref. [9], where the partial velocities and the partial angular velocities used in the derivation of Kane's equations of motion were represented by lines in Plücker coordinates [10], and this was demonstrated in the development of the equations of motion for the combined dynamics of a ship and a crane mounted on the ship.

The forces of constraint (i.e., the reaction forces) in a multibody system can be determined using Lagrange multipliers, which results in a differential–algebraic system of equations, which can be solved for the reaction forces [11,12]. This modeling approach might require stabilization [13], and the obtained reaction forces are related to the constraint equations and may need conversion to the defined coordinates. Another approach is to use a minimal set of ordinary differential equations as in Kane's formulation, where the constraint forces are eliminated from the equations. The constraint forces can then be brought to evidence using auxiliary generalized speeds, which define fictitious velocities and partial velocities in the directions of the unknown reaction forces [6]. This was investigated for a knuckleboom crane in Refs. [14,15], where the method of auxiliary generalized speeds was formulated in terms of twists and screws, which led to the systematic derivation procedure of the auxiliary partial velocities used in the determination of the constraint forces.

In this work, we extend the results of Refs. [9,14], first by deriving the equations of motion for a crane and a vessel system including a roll and pitch compensation platform between the ship deck and the crane base. Next, a procedure is developed for the determination of the reaction forces between the crane and the platform and between the platform and the vessel. A new feature of the proposed method is that the auxiliary partial velocities are given by lines in Plücker coordinates, and the reaction forces are given in terms of

[1]Corresponding author.
Contributed by the Ocean, Offshore, and Arctic Engineering Division of ASME for publication in the Journal of Offshore Mechanics and Arctic Engineering. Manuscript received November 29, 2018; final manuscript received April 29, 2019; published online June 19, 2019. Assoc. Editor: Marcelo R. Martins.

wrenches that are transformed with screw transformations. This gives a formulation with a clear geometric interpretation that is helpful in the development of the dynamical model. The performance of the derived model is studied by numerical simulations where the ship motion in waves is simulated using the JONSWAP spectrum [16–18] in combination with force response amplitude operators (RAOs) [19,20]. In addition, we investigate the efficiency of the motion compensation platform. Efficiency is evaluated in terms of the magnitude of the reaction forces at the deck/platform and platform/crane interfaces and in terms of the payload sway angles.

The rest of this article is organized as follows: Section 2 presents the theoretical preliminaries. In Sec. 3, we show the detailed derivation of the dynamical model, while in Sec. 4, we provide the procedure for the determination of reaction forces. In Secs. 5 and 6, we present the simulation results and provide the discussion of the results. Section 7 presents conclusions.

2 Preliminaries

In this section, we present the theoretical preliminaries of this work. First, we present the procedure for modeling a marine vessel in wave motion. Then, we introduce twists, which are screw representation of linear and angular velocities of rigid bodies, and wrenches, which are screw representation of forces and torques on rigid bodies. Then, we present a general method for modeling dynamics of open-chain manipulators, which is based on Kane's method, where partial angular velocities and partial linear velocities are represented as lines or screws. The modeling procedures given in the preliminaries will later be used to model a coupled crane/vessel system.

2.1 Equations of Motion of a Vessel in Waves. In this section, the mathematical model of a ship moving in waves is presented. This is done by the well-established method where force RAOs are used to calculate the wave forces on the ship and the waves are described with the JONSWAP wave spectrum [9,17]. The JONSWAP wave spectrum describes the distribution of waves in the North Sea and is given by

$$S(\omega) = 0.2053 H_s{}^2 \frac{\omega_p{}^4}{\omega^5} \exp\left[-\frac{5}{4}\left(\frac{\omega_p}{\omega}\right)^4\right]\gamma^Y \tag{1}$$

where H_s is the significant wave height, which is an approximation of the mean peak-to-peak wave height of the highest one-third of the waves, ω_p is the peak wave frequency, $\gamma = 3.3$ and

$$Y = \exp\left[-\frac{(\omega-\omega_p)^2}{2\sigma^2\omega_p^2}\right], \quad \sigma = \begin{cases} 0.07, & \text{if } \omega \le \omega_p \\ 0.09, & \text{if } \omega > \omega_p \end{cases} \tag{2}$$

The wave spectrum $S(\omega)$ is approximated with a discrete wave spectrum $S(\omega_i)$ where ω_i, $i = 1 \ldots N$, is selected randomly in the interval $[\bar{\omega}_i - \Delta\omega/2, \bar{\omega}_i + \Delta\omega/2]$, where the frequency range is divided into N equal intervals $\Delta\omega$ with a mean value $\bar{\omega}_i$ in each interval.

Short crested irregular waves are modeled by discretizing the direction χ of the waves into M equal intervals $\Delta\chi$ with a mean value $\bar{\chi}_j$ of each interval. Then, the discrete angles χ_j, $j = 1 \ldots M$, are selected randomly in each interval $[\bar{\chi}_j - \Delta\chi/2, \bar{\chi}_j + \Delta\chi/2]$, and the spreading function is set to

$$D(\chi_j) = \begin{cases} \frac{2}{\pi}\cos^2(\chi_j), & -\frac{\pi}{2} < \chi_j - \chi_0 < \frac{\pi}{2} \\ 0, & \text{otherwise} \end{cases} \tag{3}$$

where χ_0 is the dominant wave direction. The resultant wave elevation for each frequency ω_i is

$$\zeta_i(t) = \sum_{j=1}^{M} Z_{ij}\cos(\omega_i t + \epsilon_{ij}) \tag{4}$$

where ϵ_{ij} is a random phase angle and

$$Z_{ij}(t) = \sqrt{2D(\chi_j)S(\omega_i)\Delta\omega\Delta\chi} \tag{5}$$

The wave forces acting on the vessel can then be calculated using the force RAOs. The force RAO $F_k(\omega, \chi)$ for degree-of-freedom k is a transfer function, which is given in terms of its amplitude $|F(\omega, \chi)|$ and phase $\angle F(\omega, \chi)$, which are calculated from the geometry of the hull. The wave forces in the degree-of-freedom k are then determined by

$$\tau_{w,k} = \sum_{i=1}^{N}\sum_{j=1}^{M} |F_k(\omega_i, \chi_j)| Z_{ij}\cos[\omega_i t + \mu_{ij}] \tag{6}$$

where $\mu_{ij} = \epsilon_{ij} + \angle F_k(\omega_i, \chi_j)$. The equation of motion of a vessel in waves expressed in the coordinates of the vessel-fixed frame (frame 0) is given by

$$\begin{aligned} \mathbf{M}_{0,A}\dot{\boldsymbol{\nu}}_0^0 + \mathbf{D}\boldsymbol{\nu}_0^0 + \bar{\mathbf{C}}_r\mathbf{x} + \mathbf{G}\boldsymbol{\eta}_0^n &= \boldsymbol{\tau}_w + \boldsymbol{\tau}_{thr} \\ \dot{\mathbf{x}} &= \bar{\mathbf{A}}_r\mathbf{x} + \bar{\mathbf{B}}_r\boldsymbol{\nu}_0^0 \end{aligned} \tag{7}$$

where $\boldsymbol{\tau}_w = [\tau_{w,1} \ \ldots \ \tau_{w,6}]^{\mathrm{T}}$ is the vector of forces due to the force RAOs, $\mathbf{M}_{0,A} = \mathbf{M}_0 + \mathbf{A}(\infty)$, and $\mathbf{D} = \mathbf{B}(\infty)$. The matrices $\bar{\mathbf{A}}_r$, $\bar{\mathbf{B}}_r$, $\bar{\mathbf{C}}_r$ and the vector $\mathbf{x}$ are the terms from the state-space model of the fluid memory effect [21]. The term $\mathbf{M}_0$ is the associated mass matrix, $\mathbf{A}(\omega)$ is the frequency-dependent added mass matrix, $\mathbf{B}(\omega)$ is the frequency-dependent damping matrix, and $\mathbf{G}$ is the restoring force matrix [22,23]. The vector $\boldsymbol{\nu}_0^0$ is a six-dimensional vector including the linear velocity of the origin of frame 0 and the angular velocity of the vessel expressed in the vessel-fixed frame

$$\boldsymbol{\nu}_0^0 = \begin{bmatrix} \mathbf{v}_0^0 \\ \boldsymbol{\omega}_0^0 \end{bmatrix} \tag{8}$$

2.2 Definition and Properties of Screws. In this section, the necessary background in screw theory is presented [10,24,25]. Screws are used in the following sections to formulate the equations of motion with Kane's method and to calculate the reaction forces and moments. The use of screws gives a clear geometric interpretation and transformation rules that are useful in the derivation.

Consider two coordinate frames i and j, and let $\mathbf{R}_j^i$ be the rotation matrix from frame i to frame j, which satisfies $(\mathbf{R}_j^i)^{-1} = (\mathbf{R}_j^i)^{\mathrm{T}} = \mathbf{R}_i^j$. Let $\mathbf{u}^j$ be a vector given in the coordinates of j. Then, the same vector given in the coordinates of frame i will be $\mathbf{u}^i = \mathbf{R}_j^i\mathbf{u}^j$. Let $\hat{\mathbf{a}}$ denote the skew-symmetric matrix form of a vector $\mathbf{a} = [a_1 \ a_2 \ a_3]^{\mathrm{T}}$, so that

$$\hat{\mathbf{a}} = \begin{bmatrix} 0 & -a_3 & a_2 \\ a_3 & 0 & -a_1 \\ -a_2 & a_1 & 0 \end{bmatrix} \tag{9}$$

Then, $\hat{\mathbf{a}}\mathbf{b} = \mathbf{a} \times \mathbf{b}$ for any vector $\mathbf{b}$. It follows that $\hat{\mathbf{u}}^i = \mathbf{R}_j^i\hat{\mathbf{u}}^j\mathbf{R}_i^j$ [25]. Consider the screw

$$\mathbf{s}_{/B}^j = \begin{bmatrix} \mathbf{u}^j \\ \mathbf{w}^j \end{bmatrix} \tag{10}$$

which is an ordered pair of vectors $\mathbf{u}^j$ and $\mathbf{w}^j$ given in the coordinates of j and referenced to the point B. The screw will satisfy the screw transformation

$$\mathbf{s}_{/A}^i = \mathbf{U}_{AB}^i\bar{\mathbf{R}}_j^i\mathbf{s}_{/B}^j = \mathbf{V}_{AB}^{ij}\mathbf{s}_{/B}^j \tag{11}$$

where $\mathbf{s}_{/A}^i$ is given in the coordinates of i and is referenced to the point A. The screw transformation $\mathbf{V}_{AB}^{ij}$ is given in terms of screw reference transformation matrix $\mathbf{U}_{AB}^i$ from B to A and the screw

coordinate transformation matrix $\bar{\mathbf{R}}^i_j$, where

$$\mathbf{U}^i_{AB} = \begin{bmatrix} \mathbf{I} & \mathbf{0} \\ \hat{\mathbf{p}}^i_{AB} & \mathbf{I} \end{bmatrix}, \quad \bar{\mathbf{R}}^i_j = \begin{bmatrix} \mathbf{R}^i_j & \mathbf{0} \\ \mathbf{0} & \mathbf{R}^i_j \end{bmatrix} \tag{12}$$

Here, $\mathbf{p}^i_{AB}$ is the vector from A to B. It is noted that $\mathbf{U}^i_{AB}\bar{\mathbf{R}}^i_j = \bar{\mathbf{R}}^i_j\mathbf{U}^j_{AB}$, which gives the alternative expressions

$$\mathbf{V}^{ij}_{AB} = \begin{bmatrix} \mathbf{R}^i_j & \mathbf{0} \\ \hat{\mathbf{p}}^i_{AB}\mathbf{R}^i_j & \mathbf{R}^i_j \end{bmatrix} = \begin{bmatrix} \mathbf{R}^i_j & \mathbf{0} \\ \mathbf{R}^i_j\hat{\mathbf{p}}^j_{AB} & \mathbf{R}^i_j \end{bmatrix} \tag{13}$$

2.3 Lines and Screws. A line can be described by the screw

$$\mathsf{L}^i_{/A} = \begin{bmatrix} \mathbf{a}^i \\ \mathbf{m}^i_{/A} \end{bmatrix} \tag{14}$$

which is given in the coordinates of i and referenced to the point A. Here, $\mathbf{a}^i$ is the unit direction vector of the line in the coordinates of i and $\mathbf{m}^i_{/A} = \hat{\mathbf{p}}^i_A\mathbf{a}^i$ is the moment of the direction vector $\mathbf{a}^i$ about the reference point A, where $\mathbf{p}^i_A$ is the vector from A to a point on the line. The elements of the line $\mathsf{L}^i_{/A}$ are the Plücker coordinates of the line [10]. It is noted that the line $\mathsf{L}^i_{/A}$ is a screw, and it satisfies the screw transformations (11). Moreover, if the line is through the reference point A, then $\mathbf{p}^i_A = \mathbf{0}$ and $\mathsf{L}^i_{/A} = [(\mathbf{a}^i)^{\mathrm{T}}\ \mathbf{0}^{\mathrm{T}}]^{\mathrm{T}}$.

Consider the screw

$$\mathsf{s}^i_{/A} = \sigma\,\mathsf{L}^i_{/A} + \sigma\begin{bmatrix} \mathbf{0} \\ h\mathbf{a}^i \end{bmatrix} = \sigma\begin{bmatrix} \mathbf{a}^i \\ \mathbf{m}^i_{/A} + h\mathbf{a}^i \end{bmatrix} \tag{15}$$

where σ is the magnitude of the screw and h is the pitch. The line $\mathsf{L}^i_{/A}$ is said to be the screw axis of $\mathsf{s}^i_{/A}$. It is seen that if $\sigma = 1$ and $h = 0$, then $\mathsf{s}^i_{/A} = \mathsf{L}^i_{/A}$. A line is therefore said to be a screw with zero pitch. Moreover, if $h \to \infty$ and $\sigma = 1/h$, then $\mathsf{s}^i_{/A} \to \mathsf{N}^i_{/A}$, where

$$\mathsf{N}^i_{/A} = \begin{bmatrix} \mathbf{0} \\ \mathbf{a}^i \end{bmatrix} \tag{16}$$

The screw $\mathsf{N}^i_{/A}$ is therefore called a screw with infinite pitch along the unit vector $\mathbf{a}^i$.

2.4 Twists. Let the displacement from frame i to frame j be described by a translation of the origin given by a vector $\mathbf{p}^i_{ij}$ followed by a rotation $\mathbf{R}^i_j$ about the translated origin. This means that the displacement is given by the homogeneous transformation matrix

$$\mathbf{T}^i_j = \begin{bmatrix} \mathbf{R}^i_j & \mathbf{p}^i_{ij} \\ \mathbf{0}^{\mathrm{T}} & 1 \end{bmatrix} \tag{17}$$

The time derivative of the homogeneous transformation matrix is

$$\dot{\mathbf{T}}^i_j = \begin{bmatrix} \hat{\boldsymbol{\omega}}^i_{ij}\mathbf{R}^i_j & \mathbf{v}^i_{ij} \\ \mathbf{0}^{\mathrm{T}} & 0 \end{bmatrix} \tag{18}$$

where $\mathbf{v}^i_{ij}$ is the velocity of frame j relative to frame i in the coordinates of i and ω^i_{ij} is the angular velocity of j relative to i in the coordinates of i. The time derivative (18) can be written as follows [25]:

$$\dot{\mathbf{T}}^i_j = \hat{\mathsf{t}}^i_{ij/i}\mathbf{T}^i_j = \mathbf{T}^i_j\hat{\mathsf{t}}^j_{ij/j} \tag{19}$$

where

$$\hat{\mathsf{t}}^i_{ij/i} = \begin{bmatrix} \hat{\boldsymbol{\omega}}^i_{ij} & \mathbf{v}^i_{ij} + \hat{\mathbf{p}}^i_{ij}\boldsymbol{\omega}^i_{ij} \\ \mathbf{0}^{\mathrm{T}} & 0 \end{bmatrix} \quad \text{and} \quad \hat{\mathsf{t}}^j_{ij/j} = \begin{bmatrix} \hat{\boldsymbol{\omega}}^j_{ij} & \mathbf{v}^j_{ij} \\ \mathbf{0}^{\mathrm{T}} & 0 \end{bmatrix} \tag{20}$$

are the matrix forms of the screws

$$\mathsf{t}^i_{ij/i} = \begin{bmatrix} \boldsymbol{\omega}^i_{ij} \\ \mathbf{v}^i_{ij} + \hat{\mathbf{p}}^i_{ij}\boldsymbol{\omega}^i_{ij} \end{bmatrix} \quad \text{and} \quad \mathsf{t}^j_{ij/j} = \begin{bmatrix} \boldsymbol{\omega}^j_{ij} \\ \mathbf{v}^j_{ij} \end{bmatrix} \tag{21}$$

The term $\mathsf{t}^i_{ij/i}$ is called the twist of frame j relative to frame i referenced to the origin of frame i, and given in the coordinates of i, while $\mathsf{t}^j_{ij/j}$ is the same twist referenced to the origin of frame j and given in the coordinates of j. It is noted that a twist is a screw, and it satisfies the screw transformation (11). From Eq. (19), it is seen that twists in the matrix form are transformed according to

$$\hat{\mathsf{t}}^j_{ij/j} = (\mathbf{T}^i_j)^{-1}\hat{\mathsf{t}}^i_{ij/i}\mathbf{T}^i_j \tag{22}$$

Note that this transformation is only valid when the twist is given in the coordinates of the reference frame. Consider the composite displacement $\mathbf{T}^i_k = \mathbf{T}^i_j\mathbf{T}^j_k$. It follows from Eq. (19) that

$$\hat{\mathsf{t}}^j_{ij/j} = (\mathbf{T}^i_j)^{-1}\dot{\mathbf{T}}^i_j \quad \text{and} \quad \hat{\mathsf{t}}^k_{jk/k} = (\mathbf{T}^j_k)^{-1}\dot{\mathbf{T}}^j_k \tag{23}$$

which are the matrix forms of the twists

$$\mathsf{t}^j_{ij/j} = \begin{bmatrix} \boldsymbol{\omega}^j_{ij} \\ \mathbf{v}^j_{ij/j} \end{bmatrix} \quad \text{and} \quad \mathsf{t}^k_{jk/k} = \begin{bmatrix} \boldsymbol{\omega}^k_{jk} \\ \mathbf{v}^k_{jk/k} \end{bmatrix} \tag{24}$$

The twist of the composite displacement

$$\mathsf{t}^k_{ik/k} = \begin{bmatrix} \boldsymbol{\omega}^k_{ik} \\ \mathbf{v}^k_{ik/k} \end{bmatrix} \tag{25}$$

is given in the matrix form as $\hat{\mathsf{t}}^k_{ik/k} = (\mathbf{T}^i_k)^{-1}\dot{\mathbf{T}}^i_k$, which gives

$$\hat{\mathsf{t}}^k_{ik/k} = (\mathbf{T}^j_k)^{-1}(\mathbf{T}^i_j)^{-1}\dot{\mathbf{T}}^i_j\mathbf{T}^j_k + (\mathbf{T}^j_k)^{-1}\dot{\mathbf{T}}^j_k = \hat{\mathsf{t}}^k_{ij/k} + \hat{\mathsf{t}}^k_{jk/k} \tag{26}$$

where Eqs. (22) and (23) are used. It follows that

$$\mathsf{t}^k_{ik/k} = \mathsf{t}^k_{ij/k} + \mathsf{t}^k_{jk/k} \tag{27}$$

which means that the twist of a composite displacement is the sum of the twists of the individual displacements when the twists are referenced to the same point and are given in the coordinates of the same frame.

2.5 Wrenches. A wrench is a screw representation of forces and torques. The wrench with a line of action through the origin of frame i referenced to i and given in the coordinates of i is given as follows:

$$\mathsf{w}^i_{i/i} = \begin{bmatrix} \mathbf{f}^i_i \\ \mathbf{n}^i_{i/i} \end{bmatrix} \tag{28}$$

where $\mathbf{f}^i_i$ is a force and $\mathbf{n}^i_{i/i}$ is a torque. Consider the lines

$$\begin{aligned} \mathsf{L}^i_{x_i/i} &= [1\ \ 0\ \ 0\ \ 0\ \ 0\ \ 0]^{\mathrm{T}} \\ \mathsf{L}^i_{y_i/i} &= [0\ \ 1\ \ 0\ \ 0\ \ 0\ \ 0]^{\mathrm{T}} \\ \mathsf{L}^i_{z_i/i} &= [0\ \ 0\ \ 1\ \ 0\ \ 0\ \ 0]^{\mathrm{T}} \end{aligned} \tag{29}$$

referenced to the origin of frame i and given in the coordinates of i. The lines are through the origin of frame i, $\mathsf{L}^i_{x_i/i}$ is along the x_i axis, $\mathsf{L}^i_{y_i/i}$ is along the y_i axis, and $\mathsf{L}^i_{z_i/i}$ is along the z_i axis. Next, consider the screws with infinite pitch

$$\begin{aligned} \mathsf{N}^i_{x_i/i} &= [0\ \ 0\ \ 0\ \ 1\ \ 0\ \ 0]^{\mathrm{T}} \\ \mathsf{N}^i_{y_i/i} &= [0\ \ 0\ \ 0\ \ 0\ \ 1\ \ 0]^{\mathrm{T}} \\ \mathsf{N}^i_{z_i/i} &= [0\ \ 0\ \ 0\ \ 0\ \ 0\ \ 1]^{\mathrm{T}} \end{aligned} \tag{30}$$

referenced to the origin of frame i and given in the coordinates of i. Then, the wrench (28) associated with the three orthogonal forces and the three orthogonal torques can be written as a sum as follows:

$$\mathsf{w}^i_{i/i} = \sum_{j=1}^{3} \left(\mathsf{L}^i_{a_j/i} \rho_{f_j} + \mathsf{N}^i_{a_j/i} \rho_{m_j} \right) \tag{31}$$

where a_j for $j = 1, 2, 3$ stands for the axes x_i, y_i, z_i, ρ_{f_j} are the magnitudes of the forces and ρ_{m_j} are the magnitudes of the torques in x_i, y_i, z_i directions. The expression (31) can alternatively be written in the matrix form as follows:

$$\mathsf{w}^i_{i/i} = \mathbf{L}^i_{i/i} \boldsymbol{\rho} \tag{32}$$

where the columns of the matrix $\mathbf{L}^i_{i/i}$ are the screws in Eq. (31), so that

$$\mathbf{L}^i_{i/i} = \begin{bmatrix} \mathsf{L}^i_{x_i/i} & \mathsf{L}^i_{y_i/i} & \mathsf{L}^i_{z_i/i} & \mathsf{N}^i_{x_i/i} & \mathsf{N}^i_{y_i/i} & \mathsf{N}^i_{z_i/i} \end{bmatrix} \tag{33}$$

and $\boldsymbol{\rho}$ is the vector of the magnitudes of forces and torques

$$\boldsymbol{\rho} = \begin{bmatrix} \rho_{f_1} & \rho_{f_2} & \rho_{f_3} & \rho_{m_1} & \rho_{m_2} & \rho_{m_3} \end{bmatrix}^{\mathrm{T}} \tag{34}$$

Since all the columns of Eq. (33) are screws, it follows that the matrix $\mathbf{L}^i_{i/i}$ will satisfy the screw transformation. The matrix $\mathbf{L}^i_{i/i}$ can be referenced to the center of gravity (COG) of body j and expressed in the coordinates of j by

$$\mathbf{L}^j_{i/m_j} = \mathbf{V}^{ji}_{m_j,i} \mathbf{L}^i_{i/i} \tag{35}$$

where $\mathbf{V}^{ji}_{m_j,i}$ is a screw transformation matrix. The wrench (32) referenced to the COG of body j and given in the coordinates of j can then be found by

$$\mathsf{w}^j_{i/m_j} = \mathbf{L}^j_{i/m_j} \boldsymbol{\rho} \tag{36}$$

Suppose that the wrench w^j_{i/m_j} is acting on a rigid body i that is moving with a twist t^j_{ni/m_j}. Then, the power of the wrench on the twist is

$$\mathcal{P} = \left(\mathsf{w}^j_{i/m_j} \right)^{\mathrm{T}} \boldsymbol{\Pi} \, \mathsf{t}^j_{ni/m_j} \tag{37}$$

where $\boldsymbol{\Pi}$ is the interchange operator [10] defined by

$$\boldsymbol{\Pi} = \begin{bmatrix} \mathbf{0} & \mathbf{I} \\ \mathbf{I} & \mathbf{0} \end{bmatrix} \tag{38}$$

If $\left(\mathsf{w}^j_{i/m_j} \right)^{\mathrm{T}} \boldsymbol{\Pi} \mathsf{t}^j_{ni/m_j} = 0$, the twist and the wrench are said to be reciprocal.

3 Dynamic Modeling

3.1 Equation of Motion of a Serial Manipulator. Dynamics of a crane can be modeled in the same manner as dynamics of a robotic manipulator arm. Therefore, in this section, we present the detailed procedure for deriving the equations of motion for robotic manipulator arms, which is based on Ref. [14]. The equation of motion of a rigid link i is derived using the Newton–Euler approach. We describe dynamics about the COG and formulate equations in a convenient matrix form

$$\begin{bmatrix} \mathbf{M}^i_{m_i} \dot{\boldsymbol{\omega}}^i_{ni} + \hat{\boldsymbol{\omega}}^i_{ni} \mathbf{M}^i_{m_i} \boldsymbol{\omega}^i_{ni} - \mathbf{n}^i_{i/m_i} - \mathbf{n}^{i(c)}_{i/m_i} \\ m_i (\dot{\mathbf{v}}^i_{ni/m_i} + \hat{\boldsymbol{\omega}}^i_{ni} \mathbf{v}^i_{ni/m_i}) - \mathbf{f}^i_{m_i} - \mathbf{f}^{i(c)}_{m_i} \end{bmatrix} = \mathbf{0} \tag{39}$$

where $\mathbf{v}^i_{ni/m_i}$ is the linear velocity of the COG of link i relative to the inertial frame, $\boldsymbol{\omega}^i_{ni}$ is the angular velocity of link i relative to the inertial frame, and $\mathbf{M}^i_{m_i}$ is the inertia tensor of link i. The external force $\mathbf{f}^i_{m_i}$ and external moment $\mathbf{n}^i_{i/m_i}$ are applied at the COG of link i, $\mathbf{f}^{i(c)}_{m_i}$, and $\mathbf{n}^{i(c)}_{i/m_i}$ are the forces and moments of constraint. All terms are given in the coordinates of frame i, which is fixed in link i.

The twist of link i relative to the inertial frame n and expressed in the coordinates of i is given by

$$\mathsf{t}^i_{ni/i} = \begin{bmatrix} \boldsymbol{\omega}^i_{ni} \\ \mathbf{v}^i_{ni/i} \end{bmatrix} \tag{40}$$

where the twist is referenced to the origin of frame i and is given in the coordinates of i. This means that $\mathbf{v}^i_{ni/i}$ is the velocity of the origin of frame i. This twist can be transformed, so that it is referenced to the COG point m_i of link i with the transformation

$$\mathsf{t}^i_{ni/m_i} = \mathbf{U}^i_{m_i,i} \mathsf{t}^i_{ni/i} = \begin{bmatrix} \boldsymbol{\omega}^i_{ni} \\ \mathbf{v}^i_{ni/m_i} \end{bmatrix} \tag{41}$$

where $\mathbf{v}^i_{ni/m_i}$ is the velocity of the COG of link i. The matrix $\mathbf{U}^i_{m_i,i}$ is the screw reference transformation matrix (12)

$$\mathbf{U}^i_{m_i,i} = \begin{bmatrix} \mathbf{I} & \mathbf{0} \\ \hat{\mathbf{p}}^i_{m_i,i} & \mathbf{I} \end{bmatrix} \tag{42}$$

where $\mathbf{p}^i_{m_i,i}$ is the vector from the COG of link i to the origin of frame i in the coordinates of i. In the same way, the twist (40) can be referenced to the origin of frame $i+1$, which is fixed in link $i+1$, through the transformation

$$\mathsf{t}^i_{ni/i+1} = \mathbf{U}^i_{i+1,i} \mathsf{t}^i_{ni/i} \tag{43}$$

The twist (43) can be expressed in the coordinates of frame $i+1$ by the screw coordinate transformation

$$\mathsf{t}^{i+1}_{ni/i+1} = \bar{\mathbf{R}}^{i+1}_i \mathsf{t}^i_{ni/i+1} \tag{44}$$

where the screw coordinate transformation matrix (12) is

$$\bar{\mathbf{R}}^{i+1}_i = \begin{bmatrix} \mathbf{R}^{i+1}_i & \mathbf{0} \\ \mathbf{0} & \mathbf{R}^{i+1}_i \end{bmatrix} \tag{45}$$

and $\mathbf{R}^{i+1}_i$ is the orthogonal rotation matrix from $i+1$ to i. The screw transformation for the twist (40) to be referenced to the COG of link $i+1$ and to be given in the coordinates of $i+1$ can then be written as follows:

$$\mathsf{t}^{i+1}_{ni/m_{i+1}} = \mathbf{U}^{i+1}_{m_{i+1},i+1} \bar{\mathbf{R}}^{i+1}_i \mathbf{U}^i_{i+1,i} \mathsf{t}^i_{ni/i} = \mathbf{V}^{i+1,i}_{m_{i+1},i} \mathsf{t}^i_{ni/i} \tag{46}$$

where the screw transformation matrix is

$$\mathbf{V}^{i+1,i}_{m_{i+1},i} = \begin{bmatrix} \mathbf{R}^{i+1}_i & \mathbf{0} \\ \hat{\mathbf{p}}^{i+1}_{m_{i+1},i+1} \mathbf{R}^{i+1}_i + \mathbf{R}^{i+1}_i \hat{\mathbf{p}}^i_{i+1,i} & \mathbf{R}^{i+1}_i \end{bmatrix} \tag{47}$$

The twist of link $i+1$ relative to frame n can be calculated recursively from the twist of link i according to

$$\mathsf{t}^{i+1}_{n,i+1/m_{i+1}} = \mathsf{t}^{i+1}_{ni/m_{i+1}} + \mathsf{t}^{i+1}_{i,i+1/m_{i+1}} \tag{48}$$

Note that the twists in the recursive calculation scheme must be referenced to the same point and expressed in the coordinates of the same frame.

The links are connected with joints of a single rotational degree-of-freedom. The axis of rotation of the joint between link $i-1$ and link i passes through the origin of frame i. This means that the twist of link i relative to link $i-1$ will be given as a rotation about a line that passes through the origin of frame i. Then, the twist of frame i relative to $i-1$ with the reference to i and given in the coordinates of i is

$$\mathsf{t}^i_{i-1,i/i} = u_i \mathsf{L}^i_{i/i} \tag{49}$$

where the line $\mathsf{L}^i_{i/i}$ is the line of joint i and u_i is the generalized speed of joint i. The line of the joint j L^i_{j/m_i} referenced to the COG of link i

and expressed in the coordinates of i is

$$\mathsf{L}^{i}_{j/m_i} = \mathbf{V}^{ij}_{m_i,j}\mathsf{L}^{j}_{j/j} \tag{50}$$

The projection matrix of each link in the system is defined as follows:

$$\mathbf{P}_i = \begin{bmatrix} \mathsf{L}^{i}_{1/m_i} & \dots & \mathsf{L}^{i}_{i/m_i} & \mathbf{0}_{6\times(n_q-i)} \end{bmatrix} \tag{51}$$

where n_q is a number of links. The twist of link i relative to the inertial frame, referenced to the COG of link i and expressed in the coordinates of i, can be given as a sum as follows:

$$\mathsf{t}^{i}_{ni/m_i} = \sum_{j=1}^{i} u_j \mathsf{L}^{i}_{j/m_i} \tag{52}$$

The twist (52) can be expressed by the projection matrix (51) as

$$\mathsf{t}^{i}_{ni/m_i} = \mathbf{P}_i\mathbf{u} \tag{53}$$

where $\mathbf{u}$ is a vector of generalized speeds, where the elements u_i are given in Eq. (49). The derivative of (53) is given by

$$\dot{\mathsf{t}}^{i}_{ni/m_i} = \mathbf{P}_i\dot{\mathbf{u}} + \dot{\mathbf{P}}_i\mathbf{u} \tag{54}$$

where the derivative of projection matrix $\dot{\mathbf{P}}_i$ with respect to time is defined as

$$\dot{\mathbf{P}}_i = \begin{bmatrix} \dot{\mathsf{L}}^{i}_{1/m_i} & \dots & \dot{\mathsf{L}}^{i}_{i/m_i} & \mathbf{0}_{6\times(n_q-i)} \end{bmatrix} \tag{55}$$

The derivative of joint j line referenced to the COG of link i and expressed in the coordinates of i is defined as

$$\dot{\mathsf{L}}^{i}_{j/m_i} = \bar{\mathbf{d}}^{i}_{ji}\mathsf{L}^{i}_{j/m_i} \tag{56}$$

where $\bar{\mathbf{d}}^{i}_{ji}$ is the differentiation operator defined as

$$\bar{\mathbf{d}}^{i}_{ji} = \begin{bmatrix} \hat{\boldsymbol{\omega}}^{i}_{ij} & \mathbf{0} \\ -\hat{\boldsymbol{\upsilon}}^{i}_{m_i,j} & \hat{\boldsymbol{\omega}}^{i}_{ij} \end{bmatrix} \tag{57}$$

The skew-symmetric auxiliary velocity term $\hat{\boldsymbol{\upsilon}}^{i}_{m_i,j}$ is defined in a vector form as

$$\boldsymbol{\upsilon}^{i}_{m_i,j} = \hat{\boldsymbol{\omega}}^{i}_{ij}\mathbf{p}^{i}_{m_i,i} + \sum_{k=1}^{i-j-1} \hat{\boldsymbol{\omega}}^{i}_{i-k,j}\mathbf{p}^{i}_{i-k+1,i-k} \tag{58}$$

where $\mathbf{p}^{i}_{m_i,i}$ is a distance vector from the link COG point m_i to the origin of frame i, $\mathbf{p}^{i}_{i-k+1,i-k}$ is a distance vector from frame $i-k+1$ to frame $i-k$, and $\hat{\omega}^{i}_{ij}$ is a skew-symmetric form of the angular velocity of frame j with respect to frame i, all expressed in the coordinates of i. The equations of motion for link i (39) can be written as follows:

$$\mathbf{D}_i\dot{\mathsf{t}}^{i}_{ni/m_i} + \mathbf{W}_i\mathbf{D}_i\mathsf{t}^{i}_{ni/m_i} = \mathbf{\Pi}\mathsf{w}^{i(c)}_{i/m_i} + \mathbf{\Pi}\mathsf{w}^{i}_{i/m_i} \tag{59}$$

where $\mathsf{w}^{i(c)}_{i/m_i}$ and w^{i}_{i/m_i} are the wrenches of constraint and external forces, respectively. The mass matrix of link i and the auxiliary skew-symmetric matrix $\mathbf{W}_i$ are given by

$$\mathbf{D}_i = \begin{bmatrix} \mathbf{M}^{i}_{m_i} & \mathbf{0} \\ \mathbf{0} & m_i\mathbf{I} \end{bmatrix} \quad \text{and} \quad \mathbf{W}_i = \begin{bmatrix} \hat{\boldsymbol{\omega}}^{i}_{ni} & \mathbf{0} \\ \mathbf{0} & \hat{\boldsymbol{\omega}}^{i}_{ni} \end{bmatrix} \tag{60}$$

where $\mathbf{M}^{i}_{m_i}$ is the inertia tensor at the COG of link i, m_i is the mass of link i, and $\hat{\omega}^{i}_{ni}$ is the skew-symmetric form of the angular velocity vector taken from the first three rows of t^{i}_{ni/m_i}. According to the D'Alembert's principle and the principle of virtual work, constraint forces are cancelled from the equation of motion of the whole multibody system

$$\sum_i \mathbf{P}^{\mathrm{T}}_i\mathbf{\Pi}\mathsf{w}^{i(c)}_{i/m_i} = 0 \tag{61}$$

The vector of generalized external forces is given by

$$\boldsymbol{\tau}_s = \sum_i \mathbf{P}^{\mathrm{T}}_i\mathbf{\Pi}\mathsf{w}^{i}_{i/m_i} \tag{62}$$

The equation of motion of the entire multibody system is then formulated as

$$\sum_i \mathbf{P}^{\mathrm{T}}_i\left(\mathbf{D}_i\dot{\mathsf{t}}^{i}_{ni/m_i} + \mathbf{W}_i\mathbf{D}_i\mathsf{t}^{i}_{ni/m_i}\right) = \boldsymbol{\tau}_s \tag{63}$$

where the substitution of Eqs. (53) and (54) leads to the new formulation in a matrix form

$$\mathbf{M}_s\dot{\mathbf{u}} + \mathbf{C}_s\mathbf{u} = \boldsymbol{\tau}_s \tag{64}$$

where the mass and Coriolis force matrices are

$$\begin{aligned} \mathbf{M}_s &= \sum_i \mathbf{P}^{\mathrm{T}}_i\mathbf{D}_i\mathbf{P}_i \\ \mathbf{C}_s &= \sum_i \mathbf{P}^{\mathrm{T}}_i\left[\mathbf{D}_i\dot{\mathbf{P}}_i + \mathbf{W}_i\mathbf{D}_i\mathbf{P}_i\right] \end{aligned} \tag{65}$$

It is noted that the mass and Coriolis force matrices have the property that $(\dot{\mathbf{M}} - 2\mathbf{C})$ is a skew-symmetric matrix [26].

3.2 Kinematics of a Crane/Vessel System. We consider a mechanical system given in Fig. 1. The system is a knuckleboom crane with a pitch and roll compensation platform mounted on a vessel in wave motion. The system is described as a serial-link mechanism with eight links, representing the rigid bodies of the system. Body 0 is the vessel, bodies 1 and 2 describe the motion compensation platform, body 3 is the crane king, body 4 is the first boom, body 5 is the second boom, and bodies 6 and 7 describe the payload. Relative motion between bodies i and $i+1$ is modeled with single degree-of-freedom joints. Each body i has a body-fixed frame i and a mass m_i. The COG of body i for $i = 1\dots7$ is located at a distance d_i from the origin of frame i.

The position and orientation of frame 0 relative to frame n (the inertial frame) is given by the vector

$$\boldsymbol{\eta}^{n}_{0} = [x_0\ y_0\ z_0\ \phi\ \theta\ \psi]^{\mathrm{T}} \tag{66}$$

where $[x_0\ y_0\ z_0]^{\mathrm{T}}$ is the position of the origin of frame 0, ϕ is the roll angle, θ is the pitch angle, and ψ is the yaw angle. The rotation matrix from frame n to frame 0 is

$$\mathbf{R}^{n}_{0} = \mathbf{R}_z(\psi)\mathbf{R}_y(\theta)\mathbf{R}_x(\phi) \tag{67}$$

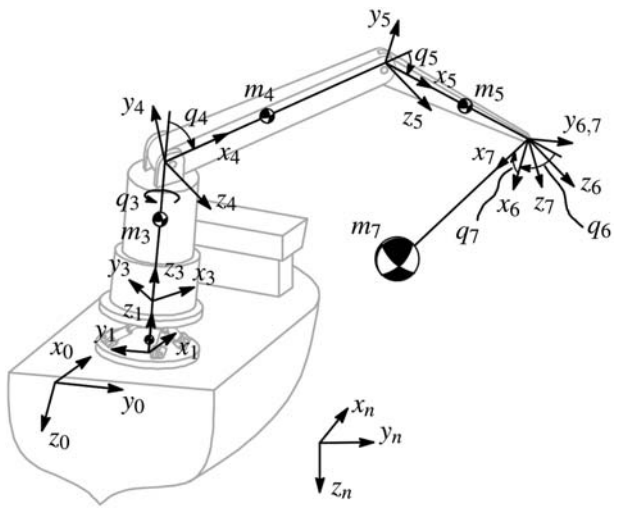

Fig. 1 A knuckleboom crane with a base motion compensation platform mounted on a vessel

where $\mathbf{R}_z(\psi)$ is the rotation matrix for rotation ψ about the z axis, $\mathbf{R}_y(\theta)$ is the rotation matrix for rotation θ about the y axis, and $\mathbf{R}_x(\phi)$ is the rotation matrix for rotation ϕ about the x axis. The rotation matrix from frame 0 to frame 1 is $\mathbf{R}_1^0 = \mathbf{R}_x(\pi)\mathbf{R}_x(q_1)$, where q_1 is the rotation angle about the x_1 axis. The rotation matrix from frame 1 to frame 2 is $\mathbf{R}_2^1 = \mathbf{R}_y(q_2)$, where q_2 is the rotation angle about the y_2 axis. The rotation matrix from frame 2 to frame 3 is $\mathbf{R}_3^2 = \mathbf{R}_z(q_3)$, where q_3 is the rotation angle about the z_3 axis. The rotation matrix from frame 3 to frame 4 is $\mathbf{R}_4^3 = \mathbf{R}_x(\frac{\pi}{2})\mathbf{R}_z(\frac{\pi}{2})\mathbf{R}_z(q_4)$, where q_4 is the rotation angle about the z_4 axis. The rotation matrix from frame 4 to frame 5 is $\mathbf{R}_5^4 = \mathbf{R}_z(q_5)$, where q_5 is the rotation angle about the z_5 axis. The rotation matrix from frame 5 to frame 6 is $\mathbf{R}_6^5 = \mathbf{R}_z(q_6)$, where q_6 is the rotation angle about the z_6 axis. The rotation matrix from frame 6 to frame 7 is $\mathbf{R}_7^6 = \mathbf{R}_y(q_7)$, where q_7 is the rotation angle about the y_7 axis.

The configuration of the system is given by the vector of generalized coordinates

$$\mathbf{q} = \begin{bmatrix} (\boldsymbol{\eta}_0^n)^{\mathrm{T}} & q_1 & \dots & q_7 \end{bmatrix}^{\mathrm{T}} \tag{68}$$

and the vector of generalized speeds [6] is given by

$$\mathbf{u} = \begin{bmatrix} (\mathbf{t}_{n0/0}^0)^{\mathrm{T}} & u_1 & \dots & u_7 \end{bmatrix}^{\mathrm{T}} \tag{69}$$

where $\mathbf{t}_{n0/0}^0$ is the twist of frame 0 relative to frame n referenced to the origin of frame 0 and expressed in the coordinates of frame 0 and $u_i = \dot{q}_i$. The lines of the crane joints in the system are given as

$$\begin{aligned}
&\mathsf{L}_{1/1}^1 = \begin{bmatrix} 1 & 0 & 0 & \mathbf{0}_{1\times 3} \end{bmatrix}^{\mathrm{T}}, \quad \mathsf{L}_{2/2}^2 = \begin{bmatrix} 0 & 1 & 0 & \mathbf{0}_{1\times 3} \end{bmatrix}^{\mathrm{T}},\\
&\mathsf{L}_{3/3}^3 = \begin{bmatrix} 0 & 0 & 1 & \mathbf{0}_{1\times 3} \end{bmatrix}^{\mathrm{T}}, \quad \mathsf{L}_{4/4}^4 = \begin{bmatrix} 0 & 0 & 1 & \mathbf{0}_{1\times 3} \end{bmatrix}^{\mathrm{T}},\\
&\mathsf{L}_{5/5}^5 = \begin{bmatrix} 0 & 0 & 1 & \mathbf{0}_{1\times 3} \end{bmatrix}^{\mathrm{T}}, \quad \mathsf{L}_{6/6}^6 = \begin{bmatrix} 0 & 0 & 1 & \mathbf{0}_{1\times 3} \end{bmatrix}^{\mathrm{T}},\\
&\mathsf{L}_{7/7}^7 = \begin{bmatrix} 0 & 1 & 0 & \mathbf{0}_{1\times 3} \end{bmatrix}^{\mathrm{T}}
\end{aligned} \tag{70}$$

The twist $\mathbf{t}_{n0/0}^0$ referenced to the origin of frame 0, relative to frame n, and expressed in the coordinates of frame 0 is

$$\mathbf{t}_{n0/0}^0 = \begin{bmatrix} \boldsymbol{\omega}_{n0}^0 \\ \mathbf{v}_{n0/0}^0 \end{bmatrix} \tag{71}$$

The twist of body 0 can be written as a sum as follows:

$$\mathbf{t}_{n0/0}^0 = \sum_{j=1}^{3} \left[\mathsf{L}_{a_j/0}^0 (\omega_{n0}^0)_{a_j} + \mathsf{N}_{a_j/0}^0 (v_{n0/0}^0)_{a_j} \right] \tag{72}$$

where a_j for $j = 1, 2, 3$ stands for the axes x_0, y_0, and z_0, the terms $(\omega_{n0}^0)_{a_j}$ and $(v_{n0/0}^0)_{a_j}$ are the projections of ω_{n0}^0 and $\mathbf{v}_{n0/0}^0$, respectively, on a_j axis, while $\mathsf{L}_{a_j/0}^0$ and $\mathsf{N}_{a_j/0}^0$ are defined in Eqs. (29) and (30). The sum (72) can be written in a matrix form as follows:

$$\mathbf{t}_{n0/0}^0 = \mathbf{L}_{0/0}^0 \mathbf{t}_{n0/0}^0 \tag{73}$$

where the matrix $\mathbf{L}_{0/0}^0$ is

$$\mathbf{L}_{0/0}^0 = \begin{bmatrix} \mathsf{L}_{x_0/0}^0 & \mathsf{L}_{y_0/0}^0 & \mathsf{L}_{z_0/0}^0 & \mathsf{N}_{x_0/0}^0 & \mathsf{N}_{y_0/0}^0 & \mathsf{N}_{z_0/0}^0 \end{bmatrix} \tag{74}$$

Since the columns of the matrix (74) are screws, then the matrix satisfies screw transformations. The matrix $\mathbf{L}_{0/0}^0$ can be referenced to the COG of body i and expressed in the coordinates of i by the screw transformation

$$\mathbf{L}_{0/m_i}^i = \mathbf{V}_{m_i,0}^{i0} \mathbf{L}_{0/0}^0 \tag{75}$$

Similarly, the line of joint j L_{j/m_i}^i referenced to the COG of body i and expressed in the coordinates of i can be obtained by $\mathsf{L}_{j/m_i}^i = \mathbf{V}_{m_i,j}^{ij} \mathsf{L}_{j/j}^j$ as in Eq. (50). The projection matrix of body 0 is defined as

$$\mathbf{P}_0 = \begin{bmatrix} \mathbf{L}_{0/0}^0 & \mathbf{0}_{6\times n_q} \end{bmatrix} \tag{76}$$

and the projection matrix of each body i for $i = 1\dots7$ is defined as

$$\mathbf{P}_i = \begin{bmatrix} \mathbf{L}_{0/m_i}^i & \mathsf{L}_{1/m_i}^i & \dots & \mathsf{L}_{i/m_i}^i & \mathbf{0}_{6\times(n_q - i)} \end{bmatrix} \tag{77}$$

where $n_q = 7$ is the number of the crane and platform DOFs. The twist of body i referenced to the COG of body i and expressed in the coordinates of i can be given as a sum

$$\mathbf{t}_{ni/m_i}^i = \mathbf{L}_{0/m_i}^i \mathbf{t}_{n0/0}^0 + \sum_{j=1}^{i} u_j \mathsf{L}_{j/m_i}^i \tag{78}$$

The twist (78) can be expressed by the projection matrix (77) and the vector of generalized speeds (69) as $\mathbf{t}_{ni/m_i}^i = \mathbf{P}_i \mathbf{u}$, as in Eq. (53). The derivative of Eq. (78) with respect to time is then $\dot{\mathbf{t}}_{ni/m_i}^i = \mathbf{P}_i \dot{\mathbf{u}} + \dot{\mathbf{P}}_i \mathbf{u}$, as in Eq. (54), where the derivative of the projection matrix $\dot{\mathbf{P}}_0 = \mathbf{0}$ and $\dot{\mathbf{P}}_i$ for $i = 1\dots7$ is defined as

$$\dot{\mathbf{P}}_i = \begin{bmatrix} \dot{\mathbf{L}}_{0/m_i}^i & \dot{\mathsf{L}}_{1/m_i}^i & \dots & \dot{\mathsf{L}}_{i/m_i}^i & \mathbf{0}_{6\times(n_q - i)} \end{bmatrix} \tag{79}$$

The derivative of the matrix $\mathbf{L}_{0/m_i}^i$ with respect to time is

$$\dot{\mathbf{L}}_{0/m_i}^i = \bar{\mathbf{d}}_{0i}^i \mathbf{L}_{0/m_i}^i \tag{80}$$

where $\bar{\mathbf{d}}_{0i}^i$ is a differentiation operator (57). The derivative of the line $\dot{\mathsf{L}}_{j/m_i}^i$ is defined in Eq. (56).

3.3 Equations of Motion of a Crane/Vessel System.

We formulate the equation of motion for the whole system by summing up the equations of motion of separate bodies premultiplied with the transpose of projection matrices. The forces and moments of constraint are cancelled from the equation of motion for the whole system by D'Alambert's principle and the principle of virtual work as shown in Eq. (61). The equations of motion of the vessel (7) are defined in terms of $\boldsymbol{\nu}_0^0$ (8); however, in this work, we use the twist $\mathbf{t}_{n0/0}^0$ (71) to represent velocities and angular velocities of the vessel. Therefore, some of the matrices in Eq. (7) need to be rearranged before the vessel and crane models can be coupled into one system. The mass, Coriolis, and gravity force matrices are transformed as

$$\mathbf{D}_0 = \boldsymbol{\Pi}\mathbf{M}_{0,A}\boldsymbol{\Pi}, \quad \mathbf{W}_0 = \boldsymbol{\Pi}\mathbf{D}\boldsymbol{\Pi}, \quad \mathbf{G}_0 = \boldsymbol{\Pi}\mathbf{G} \tag{81}$$

where $\mathbf{M}_{0,A}$, $\mathbf{D}$, and $\mathbf{G}$ are defined in Eq. (7) and $\boldsymbol{\Pi}$ is the interchange operator (38). The terms from the state-space model of the fluid memory effect are transformed as

$$\mathbf{A}_r = \bar{\mathbf{A}}_r, \quad \mathbf{B}_r = \bar{\mathbf{B}}_r\boldsymbol{\Pi}, \quad \mathbf{C}_r = \boldsymbol{\Pi}\bar{\mathbf{C}}_r \tag{82}$$

where $\bar{\mathbf{A}}_r$, $\bar{\mathbf{B}}_r$, and $\bar{\mathbf{C}}_r$ are also defined in Eq. (7).

The mass matrix of the whole system can be found by

$$\mathbf{M} = \sum_{i=0}^{7} \mathbf{P}_i^{\mathrm{T}} \mathbf{D}_i \mathbf{P}_i \tag{83}$$

where $\mathbf{D}_0$ is given in (81) and $\mathbf{D}_i$ for $i = 1\dots7$ is defined in Eq. (60). The matrix of centrifugal and Coriolis forces is

$$\mathbf{C} = \mathbf{P}_0^{\mathrm{T}} \left[\mathbf{D}_0 \dot{\mathbf{P}}_0 + \mathbf{W}_0 \mathbf{P}_0 \right] + \sum_{i=1}^{7} \mathbf{P}_i^{\mathrm{T}} \left[\mathbf{D}_i \dot{\mathbf{P}}_i + \mathbf{W}_i \mathbf{D}_i \mathbf{P}_i \right] \tag{84}$$

where $\mathbf{W}_0$ is given in Eq. (81) and $\mathbf{W}_i$ for $i = 1\dots7$ is defined in Eq. (60). The vector of generalized gravitational and buoyancy

forces is given by

$$\boldsymbol{\tau}_g = -\mathbf{P}_0^{\mathrm{T}}\mathbf{G}_0\boldsymbol{\eta}_0^n + \sum_{i=1}^{7}\mathbf{P}_i^{\mathrm{T}}\boldsymbol{\Pi}\mathsf{w}_{i/m_i}^{i(g)} \tag{85}$$

where $\mathbf{G}_0$ is the linearized gravitational and buoyancy force matrix given in Eq. (81), the wrench $\mathsf{w}_{i/m_i}^{i(g)}$ for $i=1\ldots7$ is generally defined as

$$\mathsf{w}_{i/m_i}^{i(g)} = \begin{bmatrix} \mathbf{R}_n^i \begin{bmatrix} 0 \\ 0 \\ m_i g \end{bmatrix} \\ \mathbf{0}_{3x1} \end{bmatrix} \tag{86}$$

The vector of generalized crane and motion compensation platform control forces is given by

$$\boldsymbol{\tau}_{cont} = \sum_{i=0}^{5}\mathbf{P}_i^{\mathrm{T}}\boldsymbol{\Pi}\mathsf{w}_{i/m_i}^{i(cont)} \tag{87}$$

where $\mathsf{w}_{i/m_i}^{i(cont)}$ is a wrench of control inputs given in the coordinates of frame i and referenced to the origin of frame i for $i=0$ and referenced to the COG of body i for $i=1\ldots5$. The equations of motion for the whole system can now be written as follows:

$$\begin{aligned} &\dot{\boldsymbol{\eta}}_0^n = \mathbf{J}(\boldsymbol{\eta})\mathbf{u} \\ &\mathbf{M}\dot{\mathbf{u}} + \mathbf{C}\mathbf{u} + \mathbf{P}_0^{\mathrm{T}}\mathbf{C}_r\mathbf{x} = \boldsymbol{\tau}_g + \mathbf{P}_0^{\mathrm{T}}\boldsymbol{\Pi}\boldsymbol{\tau}_{thr} + \mathbf{P}_0^{\mathrm{T}}\boldsymbol{\Pi}\boldsymbol{\tau}_w + \boldsymbol{\tau}_{cont} \\ &\dot{\mathbf{x}} = \mathbf{A}_r\mathbf{x} + \mathbf{B}_r\mathbf{P}_0\mathbf{u} \end{aligned} \tag{88}$$

where $\mathbf{A}_r$, $\mathbf{B}_r$, and $\mathbf{C}_r$ are the auxiliary matrices from the state-space model of the fluid memory effect (82), $\boldsymbol{\tau}_{thr}$ is the wrench of thruster control inputs, and $\boldsymbol{\tau}_w$ is the wrench of wave forces estimated by Eq. (6). The term $\mathbf{J}(\boldsymbol{\eta})$ is the velocity transformation matrix [17].

4 Reaction Forces

In this section, we present the procedure for determination of reaction forces (we will, in general, refer to both forces and moments by just writing *forces*) between the vessel and the motion compensation platform (i.e., in joint 1), as well as between the platform and the crane king (i.e., in joint 3).

Define a vector of unknown magnitudes of the reaction forces

$$\boldsymbol{\rho}_{\mathbf{c}} = \begin{bmatrix} \boldsymbol{\Pi}\boldsymbol{\rho}_1 \\ \boldsymbol{\Pi}\boldsymbol{\rho}_3 \end{bmatrix} \tag{89}$$

where $\boldsymbol{\rho}_1 = [\rho_{11}\ldots\rho_{16}]^{\mathrm{T}}$ is a vector of magnitudes of the reaction forces in joint 1, $\boldsymbol{\rho}_3 = [\rho_{31}\ldots\rho_{36}]^{\mathrm{T}}$ is a vector of magnitudes of the reaction forces in joint 3, and $\boldsymbol{\Pi}$ is given in (38). In both cases, first three magnitudes are forces and last three magnitudes are moments. Auxiliary velocities and angular velocities can be expressed in terms of auxiliary twists, and then, partial auxiliary velocities and partial auxiliary angular velocities can be expressed as lines or screws. In the original formulation [6,14], the auxiliary velocities are first formulated and then partial differentiation is performed with respect to auxiliary generalized speeds. In the procedure presented in this paper, we do the derivation using lines and screws directly.

The wrench at the origin of frame 1 associated with the reaction forces and moments in joint 1 is given as

$$\mathsf{w}_{1/1}^{1(c)} = \mathbf{L}_{c1/1}^1\boldsymbol{\rho}_1 \tag{90}$$

where $\mathbf{L}_{c1/1}^1$ is a set of joint lines and screws [27] given as follows:

$$\mathbf{L}_{c1/1}^1 = \begin{bmatrix} \mathsf{L}_{x_1/1}^1 & \mathsf{L}_{y_1/1}^1 & \mathsf{L}_{z_1/1}^1 & \mathsf{N}_{x_1/1}^1 & \mathsf{N}_{y_1/1}^1 & \mathsf{N}_{z_1/1}^1 \end{bmatrix} \tag{91}$$

and $\mathsf{L}_{/1}^1$, $\mathsf{N}_{/1}^1$ are defined in Eqs. (29) and (30). Since columns of the matrix (91) are screws, then the matrix satisfies screw transformations. The matrix $\mathbf{L}_{c1/1}^1$ can be referenced to the COG of body i and expressed in the coordinates of frame i

$$\mathbf{L}_{c1/m_i}^i = \mathbf{V}_{m_i,1}^{i1}\mathbf{L}_{c1/1}^1 \tag{92}$$

Analogically, the wrench at the origin of frame 3 associated with all the reaction forces and moments in joint 3 is given as

$$\mathsf{w}_{3/3}^{3(c)} = \mathbf{L}_{c3/3}^3\boldsymbol{\rho}_3 \tag{93}$$

where $\mathbf{L}_{c3/3}^3$ is a set of joint lines and screws [27] given as

$$\mathbf{L}_{c3/3}^3 = \begin{bmatrix} \mathsf{L}_{x_3/3}^3 & \mathsf{L}_{y_3/3}^3 & \mathsf{L}_{z_3/3}^3 & \mathsf{N}_{x_3/3}^3 & \mathsf{N}_{y_3/3}^3 & \mathsf{N}_{z_3/3}^3 \end{bmatrix} \tag{94}$$

and $\mathsf{L}_{/3}^3$ and $\mathsf{N}_{/3}^3$ are also defined in Eqs. (29) and (30). The matrix $\mathbf{L}_{c3/3}^3$ can be referenced to the COG of body i and expressed in the coordinates of frame i

$$\mathbf{L}_{c3/m_i}^i = \mathbf{V}_{m_i,3}^{i3}\mathbf{L}_{c3/3}^3 \tag{95}$$

The auxiliary projection matrix of each body i in the system is defined as

$$\begin{aligned} &\mathbf{P}_{\mathbf{c}0} = \mathbf{0} \\ &\mathbf{P}_{\mathbf{c}i} = \begin{bmatrix} \mathbf{L}_{c1/m_i}^i & \mathbf{0}_{6\times6} \end{bmatrix}, \quad \text{for } i = 1, 2 \\ &\mathbf{P}_{\mathbf{c}i} = \begin{bmatrix} \mathbf{L}_{c1/m_i}^i & \mathbf{L}_{c3/m_i}^i \end{bmatrix}, \quad \text{for } i \geq 3 \end{aligned} \tag{96}$$

The auxiliary vector of generalized gravitational and buoyancy forces is given by

$$\boldsymbol{\tau}_{\mathbf{f}g} = -\mathbf{P}_{\mathbf{c}0}^{\mathrm{T}}\mathbf{G}_0\boldsymbol{\eta}_0^n + \sum_{i=1}^{7}\mathbf{P}_{\mathbf{c}i}^{\mathrm{T}}\boldsymbol{\Pi}\mathsf{w}_{i/m_i}^{i(g)} \tag{97}$$

where the terms $\mathbf{G}_0$, $\boldsymbol{\eta}_0^n$, and $\mathsf{w}_{i/m_i}^{i(g)}$ are the same as in Eq. (85). The auxiliary vector of generalized crane and motion compensation platform control forces is given by

$$\boldsymbol{\tau}_{\mathbf{f}cont} = \sum_{i=0}^{5}\mathbf{P}_{\mathbf{c}i}^{\mathrm{T}}\boldsymbol{\Pi}\mathsf{w}_{i/m_i}^{i(cont)} \tag{98}$$

where $\mathsf{w}_{i/m_i}^{i(cont)}$ is the same as in Eq. (87). The vector of the unknown magnitudes of the reaction forces can now be found by

$$\begin{aligned} \boldsymbol{\rho}_{\mathbf{c}} = \mathbf{M}_{\mathbf{f}}\dot{\mathbf{u}} + \mathbf{C}_{\mathbf{f}}\mathbf{u} + \mathbf{P}_{\mathbf{c}0}^{\mathrm{T}}\mathbf{C}_r\mathbf{x} \\ - \boldsymbol{\tau}_{\mathbf{f}g} - \mathbf{P}_{\mathbf{c}0}^{\mathrm{T}}\boldsymbol{\tau}_{thr} - \mathbf{P}_{\mathbf{c}0}^{\mathrm{T}}\boldsymbol{\tau}_w - \boldsymbol{\tau}_{\mathbf{f}cont} \end{aligned} \tag{99}$$

where the matrices $\mathbf{M}_{\mathbf{f}}$ and $\mathbf{C}_{\mathbf{f}}$ are defined as

$$\mathbf{M}_{\mathbf{f}} = \sum_{i=0}^{7}\mathbf{P}_{\mathbf{c}i}^{\mathrm{T}}\mathbf{D}_i\mathbf{P}_i \tag{100}$$

and

$$\mathbf{C}_{\mathbf{f}} = \mathbf{P}_{\mathbf{c}0}^{\mathrm{T}}\left[\mathbf{D}_0\dot{\mathbf{P}}_0 + \mathbf{W}_0\mathbf{P}_0\right] + \sum_{i=1}^{7}\mathbf{P}_{\mathbf{c}i}^{\mathrm{T}}\left[\mathbf{D}_i\dot{\mathbf{P}}_i + \mathbf{W}_i\mathbf{D}_i\mathbf{P}_i\right] \tag{101}$$

where $\mathbf{D}_0$, $\mathbf{D}_i$, $\mathbf{W}_0$, and $\mathbf{W}_i$ are the same as in Eqs. (83) and (84). Provided that $\mathbf{P}_{\mathbf{c}0} = \mathbf{0}$, then Eq. (99) is simplified to

$$\boldsymbol{\rho}_{\mathbf{c}} = \mathbf{M}_{\mathbf{f}}\dot{\mathbf{u}} + \mathbf{C}_{\mathbf{f}}\mathbf{u} - \boldsymbol{\tau}_{\mathbf{f}g} - \boldsymbol{\tau}_{\mathbf{f}cont} \tag{102}$$

where $\dot{\mathbf{u}}$ and $\mathbf{u}$ are obtained from the simulation of Eq. (88).

5 Simulation Results

The dynamical model of the marine vessel with the deck crane and the procedure for the determination of reaction forces are

Table 1 Crane dimensions (m)

Term	l_1	l_2	l_3	l_4	l_5	l_6	l_7
Value	0.01	3.0	10.0	10.0	8.0	0.01	5.0

Table 2 Crane masses (t)

Term	m_1	m_2	m_3	m_4	m_5	m_6	m_7
Value	0.01	40	70	40	30	0.01	20

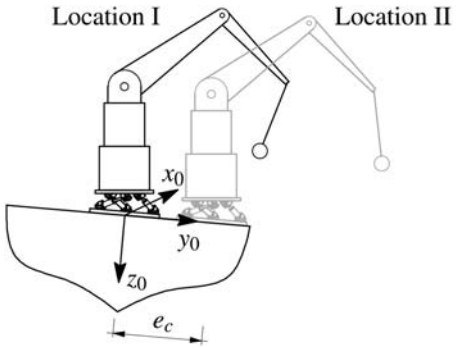

Fig. 2 Two locations of the crane considered in simulations, the offset $e_c = 3.0$ m along the y_0 axis

implemented numerically in this section. The lengths of the crane bodies are given in Table 1. The COG distances for the crane bodies are defines as $d_i = l_i/2$ for $i = 1 \ldots 6$ and $d_7 = l_7$. The masses of the crane bodies are given in Table 2.

The implemented vessel model is the same supply vessel model as used in Ref. [9]. The main vessel dimensions are as follows: the length between perpendiculars is 82.5 m, the breadth is 8.0 m, and the draught is 6.0 m. The mass of the vessel is 6362 mT. The hydrodynamic coefficients, force RAOs, parameters of the radiation force model, and rigid body mass matrix of the vessel were taken from the marine systems simulator [19]. The wave parameters considered in the simulations are significant wave height $H_s = 5$ m and peak frequency $\omega_p = 1.26$ rad/s.

The vessel is initialized at $\boldsymbol{\eta}_0^n = [0\ 0\ 0\ 0\ 0\ 0]^{\mathrm{T}}$, and a proportional-derivative (PD) controller is implemented for surge, sway, and yaw control, where the control task is to keep the controlled DOFs at zero. The crane is initialized at $q3 = -90$ deg, $q_4 = -45$ deg, $q_5 = -90$ deg, $q_6 = -45$ deg, and $q_7 = 0$ deg. We have implemented a PD controller with gravity compensation to keep q_i for $i = 3, 4, 5$ at its initial values, and the pendulum DOFs q_6, q_7 are unactuated.

The roll and pitch compensation platform is initialized at $q_1 = 0$ deg and $q_2 = 0$ deg. Two control strategies are assumed in this paper, where in both, a PD controller is implemented. The first strategy is when the motion platform is controlled to stay horizontal (mode "MC on"). The second strategy is when the motion platform is controlled to stay parallel to the vessel deck (mode "MC off"). The second control strategy is used to simulated the absence of motion compensation for the comparison purposes.

Two simulations are run with two different crane locations on the vessel deck; see Fig. 2. In location I, the crane is placed in the origin of frame 0, which is in the middle of the deck seen in the transverse section. In location II, the crane is moved along the y_0 axis by a distance of $e_c = 3.0$ m.

5.1 Crane Location I. The results of the numerical simulation of the system with the crane in location I (see Fig. 2) are presented

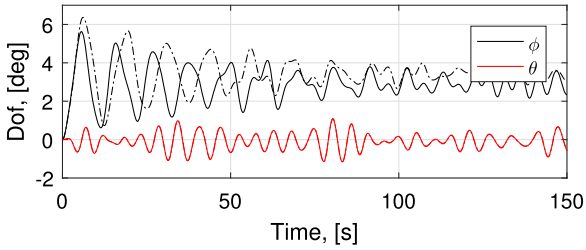

Fig. 3 Roll and pitch angles for crane location I. Solid lines show results in "MC on" mode and dashed lines in "MC off" mode. The pitch data are superposed.

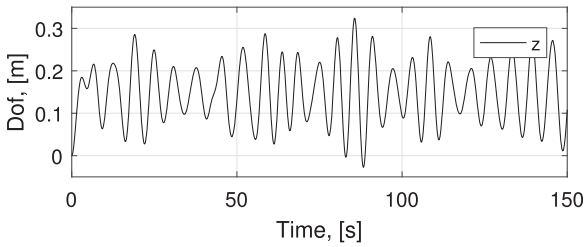

Fig. 4 Heave of the vessel for crane location I. Solid lines show results in "MC on" mode and dashed lines in "MC off" mode. The lines are superposed.

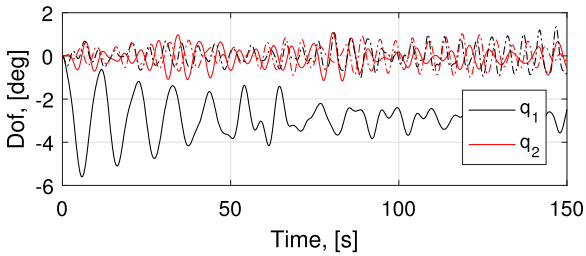

Fig. 5 DOFs of the motion compensation platform for crane location I. Solid lines show results in "MC on" mode and dashed lines in "MC off" mode.

in this section. The results in time series with an active roll and pitch compensation platform (mode "MC on") are shown as solid lines, while the results with a locked roll and pitch compensation platform (mode "MC off") are shown as dashed lines. Roll, pitch, and heave time histories are shown in Figs. 3 and 4, while surge, sway, and yaw are close to zero throughout the simulation, and those graphs are omitted. The time histories for DOFs of the roll and pitch compensation platform are shown in Fig. 5. The time histories for the payload angles θ_1 and θ_2 (see Fig. 6) are shown in Figs. 7 and 8. The reaction moments and reaction forces on platform from the deck given in the coordinates of frame 1 are shown in Figs. 9–11.

The reaction moments and reaction forces on the crane king from the platform given in the coordinates of frame 3 are shown in Figs. 12–14.

5.2 Crane Location II. The results of the numerical simulation of the system with the crane in location II (see Fig. 2) are presented in this section. The results in time series with an active roll and pitch compensation platform (mode "MC on") are shown as solid lines, while the results with a locked roll and pitch compensation platform (mode "MC off") are shown

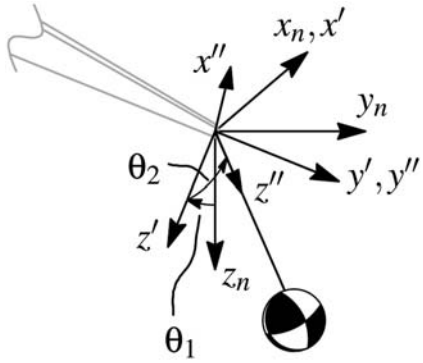

Fig. 6 Orientation of the payload is described by the rotation $R_{x_n}(\theta_1)R_{y'}(\theta_2)$ from the inertial frame

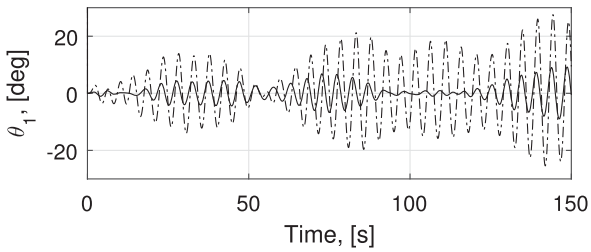

Fig. 7 Payload orientation angle θ_1 for crane location I. Solid lines show results in "MC on" mode and dashed lines in "MC off" mode.

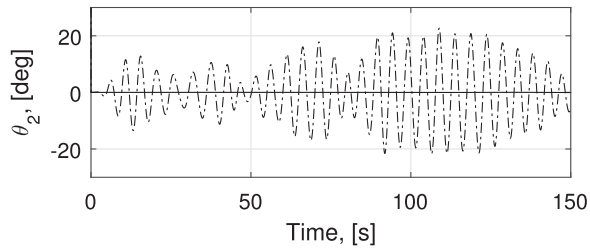

Fig. 8 Payload orientation angle θ_2 for crane location I. Solid lines show results in "MC on" mode and dashed lines in "MC off" mode.

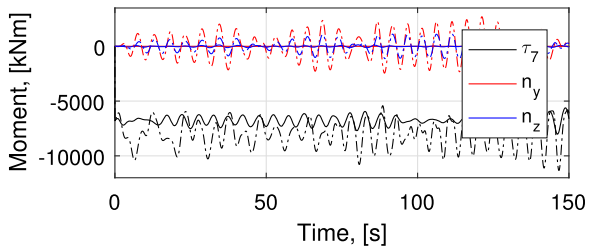

Fig. 9 Reaction moments on platform for crane location I. Solid lines show results in "MC on" mode dashed lines in "MC off" mode.

as dashed lines. Roll, pitch, and heave time histories are shown in Figs. 15 and 16, while surge, sway, and yaw are close to zero throughout the simulation, and those graphs are omitted. The time histories for DOFs of the roll and pitch compensation platform are shown in Fig. 17. The time histories for the payload angles θ_1 and θ_2 (see Fig. 6) are shown in Figs. 18 and 19. The reaction moments and reaction forces on platform from the deck are shown in Figs. 20–22.

The reaction moments and reaction forces on the crane king from the platform are shown in Figs. 23–25.

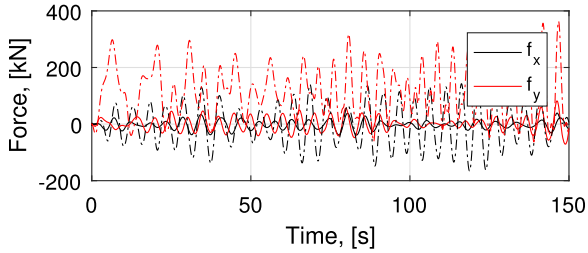

Fig. 10 Reaction forces on platform for crane location I. Solid lines show results in "MC on" mode and dashed lines in "MC off" mode.

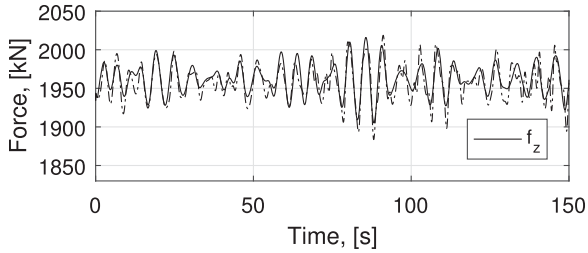

Fig. 11 Reaction force on platform for crane location I. Solid lines show results in "MC on" mode and dashed lines in "MC off" mode.

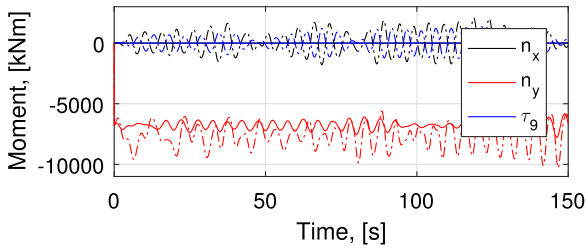

Fig. 12 Reaction moments on crane for crane location I. Solid lines show results in "MC on" mode and dashed lines in "MC off" mode.

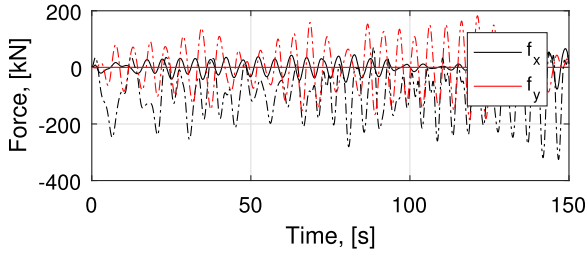

Fig. 13 Reaction forces on crane for crane location I. Solid lines show results in "MC on" mode and dashed lines in "MC off" mode.

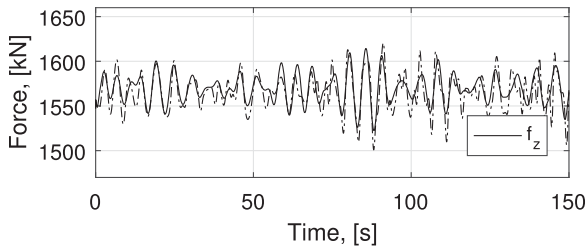

Fig. 14 Reaction force on crane for crane location I. Solid lines show results in "MC on" mode and dashed lines in "MC off" mode.

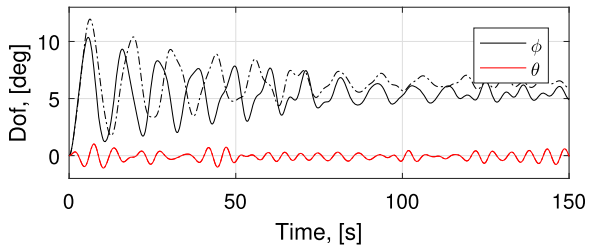

Fig. 15 Roll and pitch angles for crane location II. Solid lines show results in "MC on" mode and dashed lines in "MC off" mode. The pitch data are superposed.

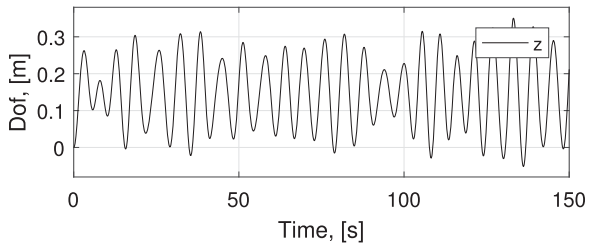

Fig. 16 Heave of the vessel for crane location II. Solid lines show results in "MC on" mode and dashed lines in "MC off" mode. The lines are superposed.

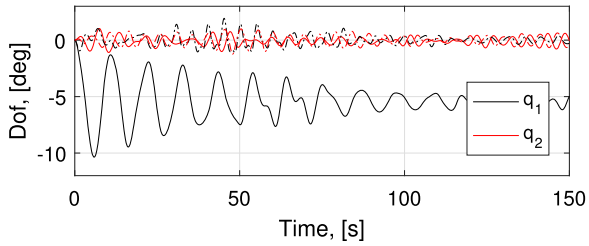

Fig. 17 DOFs of the motion compensation platform for crane location II. Solid lines show results in "MC on" mode and dashed lines in "MC off" mode.

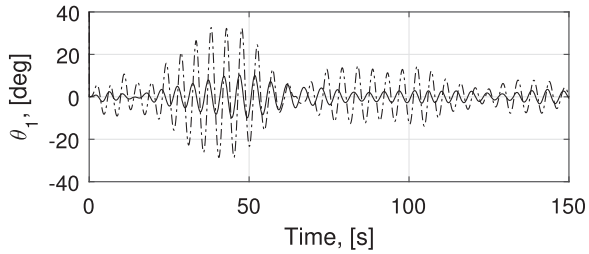

Fig. 18 Payload orientation angle θ_1 for crane location II. Solid lines show results in "MC on" mode and dashed lines in "MC off" mode.

6 Discussion of Results

In this section, we discuss the results that were presented in Sec. 5.

The comparison of the maximum values of payload angles throughout the simulation for crane locations I and II are given in Figs. 26 and 27. The active roll and pitch motion compensation platform resulted in reduction of the pendulum sway of 66.5% for θ_1 and 99.7% for θ_2 in crane location I. Reduction of the crane pendulum sway in location II for θ_1 and θ_2 is accordingly 68.5% and 97.7%.

The relative comparison of the normalized maximum values of the reaction forces and moments on the platform from the vessel deck for crane locations I and II are given in Figs. 28 and 29. The relative comparison of the normalized maximum values of the reaction forces and

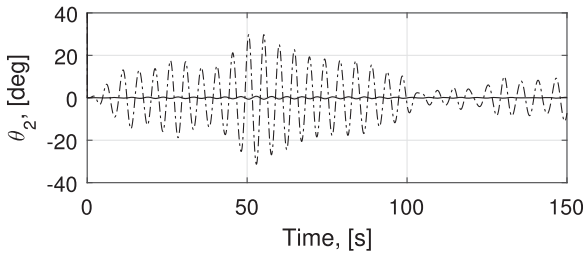

Fig. 19 Payload orientation angle θ_2 for crane location II. Solid lines show results in "MC on" mode and dashed lines in "MC off" mode.

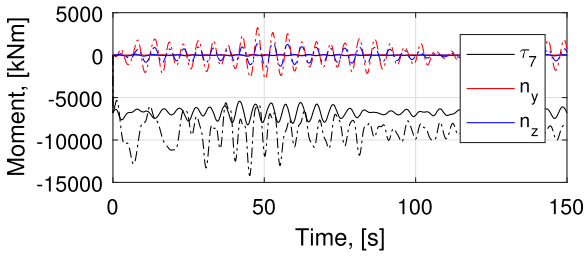

Fig. 20 Reaction moments on platform for crane location II. Solid lines show results in "MC on" mode and dashed lines in "MC off" mode.

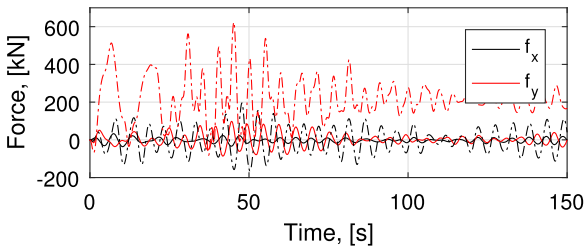

Fig. 21 Reaction forces on platform for crane location II. Solid lines show results in "MC on" mode and dashed lines in "MC off" mode.

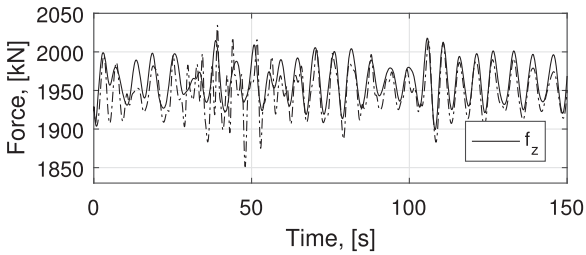

Fig. 22 Reaction force on platform for crane location II. Solid lines show results in "MC on" mode and dashed lines in "MC off" mode.

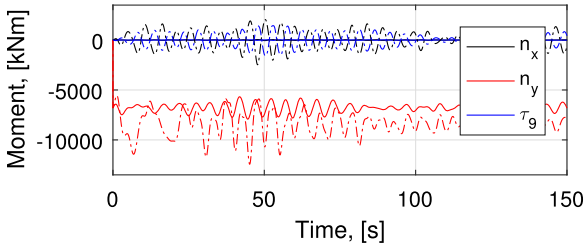

Fig. 23 Reaction moments on crane for crane location II. Solid lines show results in "MC on" mode and dashed lines in "MC off" mode.

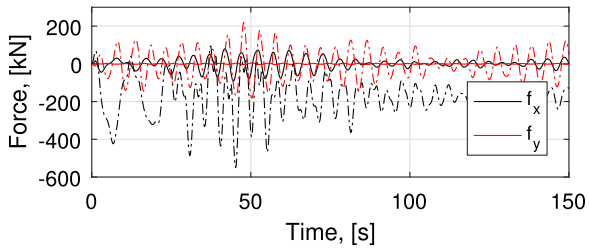

Fig. 24 Reaction forces on crane for crane location II. Solid lines show results in "MC on" mode and dashed lines in "MC off" mode.

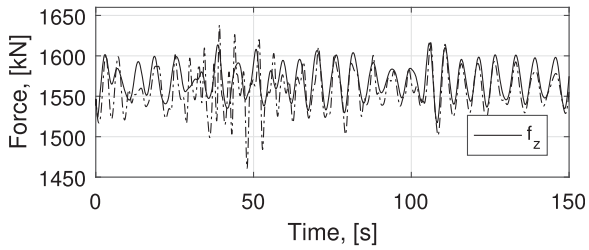

Fig. 25 Reaction force on crane for crane location II. Solid lines show results in "MC on" mode and dashed lines in "MC off" mode.

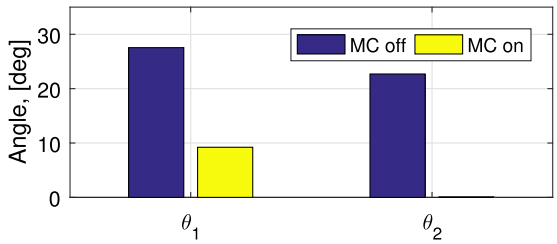

Fig. 26 Comparison of maximum values of payload orientation angles for crane location I

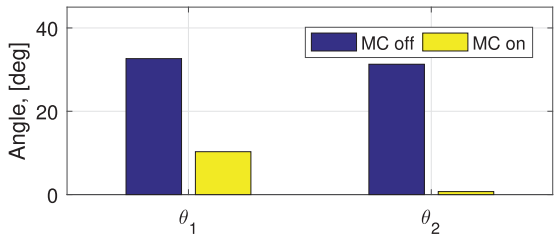

Fig. 27 Comparison of maximum values of payload orientation angles for crane location II

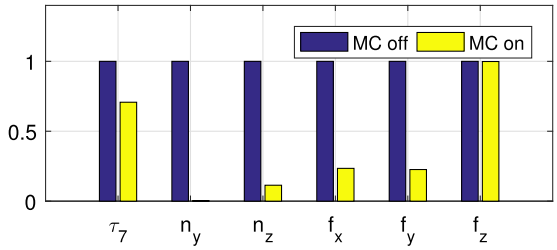

Fig. 28 Relative comparison of reaction forces and moments on the platform for crane location I

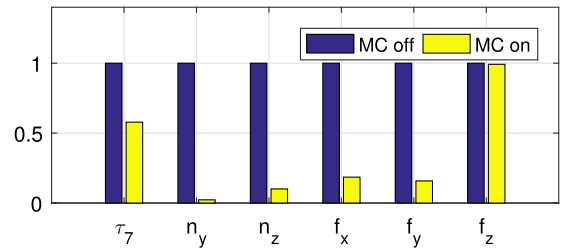

Fig. 29 Relative comparison of reaction forces and moments on the platform for crane location II

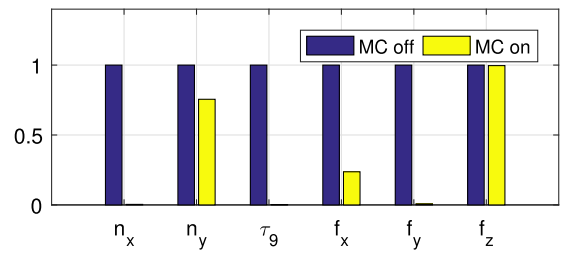

Fig. 30 Relative comparison of reaction forces and moments on the crane for crane location I

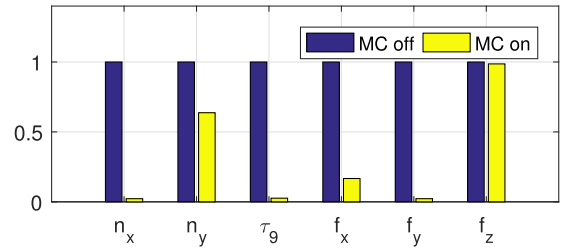

Fig. 31 Relative comparison of reaction forces and moments on the crane for crane location II

Table 3 Reduction of maximum values of reaction forces and moments on the platform due to active motion compensation, in (%)

Reaction	τ_7	n_{y_1}	n_{z_1}	f_{x_1}	f_{y_1}	f_{z_1}
Location I	29.3	99.7	88.6	76.5	77.4	0.0
Location II	42.2	97.7	90.0	81.5	84.2	0.0

Table 4 Reduction of maximum values of reaction forces and moments on the crane king due to active motion compensation, in (%)

Reaction	n_{x_3}	n_{y_3}	τ_9	f_{x_3}	f_{y_3}	f_{z_3}
Location I	99.6	24.5	99.8	76.3	99.2	0.0
Location II	97.8	36.3	97.4	83.3	97.8	0.0

moments on the crane king from the platform for crane locations I and II are given in Figs. 30 and 31. Reduction of the reaction moment and force components due to the active roll and pitch compensation platform is summed up in Tables 3 and 4.

The active roll and pitch compensation platform provided significant reduction in the maximum magnitudes of the payload sway angles, reaction forces, and reaction moments. The reduction of the

payload sway angles improves the operational weather window of the cranes, while the reduction of the reaction forces and moments leads to the benefits in structural design and fatigue lifetime.

7 Conclusions

We have presented a procedure for dynamic modeling of a coupled crane and vessel system when the vessel is moving in waves. We have included the case when a roll and pitch compensation platform is installed between the vessel and the crane. The kinematics of the model were derived by representing velocities and angular velocities of the bodies as twists and by representing partial velocities and partial angular velocities as lines in Plücker coordinates. In addition, we have presented a procedure for the determination of reaction forces in the deck/platform and platform/crane interfaces. The reaction forces were determined from algebraic relations, which were conveniently derived by representing the unknown reaction forces as wrenches. Since wrenches are screws, screw transformations were also used in the derivations.

The presented model was implemented, and the results of numerical simulations were provided. The analysis was carried out for two crane locations: in the middle of the deck and closer to the starboard. The simulation results were used to study the efficiency of a roll and pitch compensation platform installed between a crane and a vessel. The efficiency was evaluated in terms of the magnitude of the determined reaction forces and in terms of the magnitude of the payload sway angles. It was shown that the compensation of roll and pitch angles, such that the base of the crane stays horizontal, leads to significant reduction of both reaction forces and payload sway angles. The simulation results demonstrated that the proposed model can be used to determine dynamical forces for structural and fatigue analyses of the crane/vessel interface.

Further development of this work could be implementation of a crane/platform control system for damping out the payload oscillations. In addition, the crane model can be extended with a payload hoisting degree-of-freedom.

Funding Data

- Norwegian Research Council, SFI Offshore Mechatronics, Project No. 237896

References

[1] Schellin, T., Jiang, T., and Sharma, S., 1991, "Crane Ship Response to Wave Groups," ASME J. Offshore Mech. Arct. Eng., **113**(3), pp. 211–218.

[2] Chu, Y., Hatledal, L. I., Æsøy, V., Ehlers, S., and Zhang, H., 2018, "An Object-Oriented Modeling Approach to Virtual Prototyping of Marine Operation Systems Based on Functional Mock-Up Interface Co-Simulation," ASME J. Offshore Mech. Arct. Eng., **140**(2), p. 021601.

[3] Blochwitz, T., Otter, M., Akesson, J., Arnold, M., Clau, C., Elmqvist, H., Friedrich, M., Junghanns, A., Mauss, J., Neumerkel, D., Olsson, H., and Viel, A., 2012, "Functional Mockup Interface 2.0: The Standard for Tool Independent Exchange of Simulation Models," Proceedings of the 9th International Modelica Conference, Munich, Germany, Sept. 3–5, pp. 173–184.

[4] From, P. J., Gravdahl, J. T., and Pettersen, K. Y., 2014, *Vehicle-Manipulator Systems: Modeling for Simulation, Analysis, and Control*, Springer, New York.

[5] Egeland, O., and Sagli, J. R., 1993, "Coordination of Motion in a Spacecraft/Manipulator System," Int. J. Rob. Res., **12**(4), pp. 366–379.

[6] Kane, T. R., and Levinson, D. A., 1985, *Dynamics, Theory and Applications*, McGraw-Hill, New York.

[7] Kane, T. R., and Levinson, D. A., 1983, "The Use of Kane's Dynamical Equations in Robotics," Int. J. Rob. Res., **2**(3), pp. 3–21.

[8] Angeles, J., and Ma, O., 1988, "Dynamic Simulation of *n*-Axis Serial Robotic Manipulators Using a Natural Orthogonal Complement," Int. J. Rob. Res., **7**(5), pp. 32–47.

[9] Tysse, G. O., and Egeland, O., 2018, "Dynamic Interaction of a Heavy Crane and a Ship in Wave Motion," J. Model. Identif. Control, **39**(2), pp. 45–60.

[10] McCarthy, J. M., and Soh, G. S., 2011, *Geometric Design of Linkages*, Springer Verlag, Berlin.

[11] Shabana, A. A., 2013, *Dynamics of Multibody Systems*, Cambridge University Press, Cambridge.

[12] Huston, R., 1999, "Constraint Forces and Undetermined Multipliers in Constrained Multibody Systems," Multibody Syst. Dyn., **3**(4), pp. 381–389.

[13] Marques, F., Souto, A. P., and Flores, P., 2017, "On the Constraints Violation in Forward Dynamics of Multibody Systems," Multibody Syst. Dyn., **39**(4), pp. 385–419.

[14] Cibicik, A., and Egeland, O., 2018, "Determination of Constraint Forces for an Offshore Crane on a Moving Base," 2018 5th International Conference on Control, Decision and Information Technologies (CoDIT), Thessaloniki, Greece, Apr. 10–13, pp. 233–240.

[15] Cibicik, A., and Egeland, O., 2019, "Dynamic Modelling and Force Analysis of a Knuckle Boom Crane Using Screw Theory," Mech. Mach. Theory, **133**, pp. 179–194.

[16] Hasselmann, K., Barnett, T., Bouws, E., Carlson, H., Cartwright, D., Enke, K., Ewing, J., Gienapp, H., Hasselmann, D., Kruseman, P., Meerburg, A., Muller, P., Olbers, D., Richter, K., Sell, W., and Walden, H., 1973, "Measurements of Wind-Wave Growth and Swell Decay During the Joint North Sea Wave Project (JONSWAP)," Deutches Hydrographisches Institut, Ergänzungsheft 8–12.

[17] Fossen, T. I., 2011, *Handbook of Marine Craft Hydrodynamics and Motion Control*, John Wiley & Sons, New York.

[18] DNV GL, 2017, "Environmental Conditions and Environmental Loads," Recommended Practice—DNVGL-RP-C205, DNV GL AS.

[19] Perez, T., Fossen, T. I., and Sørensen, A., 2004, "A Discussion About Seakeeping and Manoeuvring Models for Surface Vessels," Centre for Ships and Ocean Structures (CESOS), Technical Report No. MSS-TR-001.

[20] Perez, T., and Fossen, T. I., 2007, "Kinematic Models for Manoeuvring and Seakeeping of Marine Vessels," J. Model. Identif. Control, **28**(1), pp. 19–30.

[21] Kristiansen, E ., Hjulstad, Å., and Egeland, O., 2005, "State-Space Representation of Radiation Forces in Time-Domain Vessel Models," Ocean Eng., **32**(17–18), pp. 2195–2216.

[22] Smogeli, Ø., Perez, T., Fossen, T., and Sørensen, A., 2005, "The Marine Systems Simulator State-Space Model Representation for Dynamically Positioned Surface Vessels," International Maritime Association of the Mediterranean IMAM Conference, Lisbon, Portugal, Sept. 26–30, pp. 748–757.

[23] Ross, A., Perez, T., and Fossen, T. I., 2006, "Clarification of the Low-Frequency Modelling Concept for Marine Craft," 7th IFAC Conference on Manoeuvring and Control of Marine Vessels MCMC, Portugal, Sept. 20–22.

[24] Angeles, J., 2014, *Fundamentals of Robotic Mechanical Systems: Theory, Methods, and Algorithms*, 4th ed., Springer, New York.

[25] Murray, R. M., Sastry, S. S., and Zexiang, L., 1994, *A Mathematical Introduction to Robotic Manipulation*, 1st ed., CRC Press, Inc., Boca Raton, FL.

[26] Siciliano, B., Sciavicco, L., Villani, L., and Oriolo, G., 2010, *Robotics: Modelling, Planning and Control*, Springer Science & Business Media, Berlin.

[27] Davidson, J. K., Hunt, K. H., and Hunt, K. H., 2004, *Robots and Screw Theory: Applications of Kinematics and Statics to Robotics*, Oxford University Press, Oxford.